NMO stretch in survey design and processing

Gijs J. O. Vermeer, *3DSymSam – Geophysical Advice*

Introduction

In seismic survey design the maximum acceptable stretch factor is often used as a basis for computation of the mute offset, and ultimately, for the choice of maximum offset of the geometry (Vermeer, 2012). The formula that is commonly used does not take the dependence of the rms-velocity $V_{\rm rms}$ on zero-offset time t_0 into account. In this note (serving as an alternative to Section 4.4.6 in Vermeer, 2012) a more accurate formula is derived and discussed. It turns out that stretch tends to increase faster as function of offset than according to the old formula. As a consequence shorter offsets may be selected that satisfy maximum stretch requirements. A most interesting consequence of the new approach is that the new formula for mute offset computed for stretch S predicts the offset corresponding to incidence angle i according to $S = 1/\cos i$.

What maximum stretch factor is acceptable depends on the acceptable average stretch factor of all data stacked together. This average stretch determines the resolution of the final stacked and migrated data. Formulas for average stretch for 2D and 3D data are derived and are linked to the maximum stretch factor. Average stretch also depends on the variation of $V_{\rm rms}$ with t_0; however, this dependence is not very strong and earlier conclusions (Section 4.4.6.3 in Vermeer, 2012) about average stretch for 2D data compared to 3D data remain valid to a large extent.

NMO stretch factor

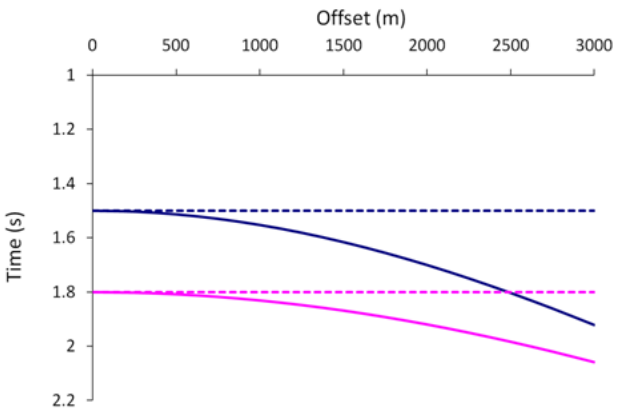

Figure 1 The NMO correction aligns reflections at zero-offset time. This causes NMO stretch.

The NMO stretch factor is the factor with which offset data are stretched to match the zero-offset data. Figure 1 gives a pictorial description of the NMO stretch factor. Assuming that reflection time t as a function of offset X can be described by a hyperbola $t^2 = t_0^2 + X^2/V_{\rm rms}^2$ with t_0 is zero-offset time and $V_{\rm rms}$ is rms velocity, the stretch factor S can be derived as (Vermeer, 1990)

$$S = \frac{{\rm d}t_0}{{\rm d}t} = \frac{t}{t_0}\Big/\left(1 - \frac{X^2}{t_0 V_{rms}^3}\frac{{\rm d}V_{\rm rms}}{{\rm d}t_0}\right) = \sqrt{1+\xi^2}\,/(1-\xi^2\psi), \quad (1)$$

where $\xi = \dfrac{X}{V_{\rm rms}t_0}$ and $\psi = \dfrac{t_0}{V_{rms}}\dfrac{{\rm d}V_{\rm rms}}{{\rm d}t_0}$. This derivation takes the dependence of $V_{\rm rms}$ on time into account.

Equation 1 shows that the stretch factor increases with offset and decreases with increasing rms-velocity and zero-offset time. A stretch factor of say 1.15 increases the length of a wavelet with 15% and decreases all frequencies in the wavelet with the same percentage. Therefore, the NMO stretch reduces the maximum frequency in offset data and it reduces resolution. To limit the loss of high frequencies, a maximum stretch factor may be selected in processing. This same maximum stretch factor may be used in survey design to estimate the range of useful offsets as a function of time.

In a constant velocity medium, $\psi = 0$, and $S = \sqrt{1+\xi^2}$. This is the formula that was commonly used earlier to relate mute offset to maximum stretch factor S_{max}.

Maximum stretch factor, mute function, and angle of incidence

Equation 1 can be used to compute the mute offset X_{mute} corresponding to a given maximum stretch factor S_{max} from a given velocity function:

$$X_{mute} = V_{rms} t_0 \sqrt{\frac{1}{\psi} + \frac{1}{2\psi^2 S_{max}^2}\left(1 - \sqrt{4S_{max}^2(\psi^2+\psi)+1}\right)} \quad \left(\psi \neq 0 \text{ and } \psi > \frac{-S_{max}^2 + \sqrt{S_{max}^4 - S_{max}^2}}{2S_{max}^2}\right) \quad (2)$$

$$X_{mute} = V_{rms} t_0 \sqrt{S_{max}^2 - 1} \quad (\psi = 0)$$

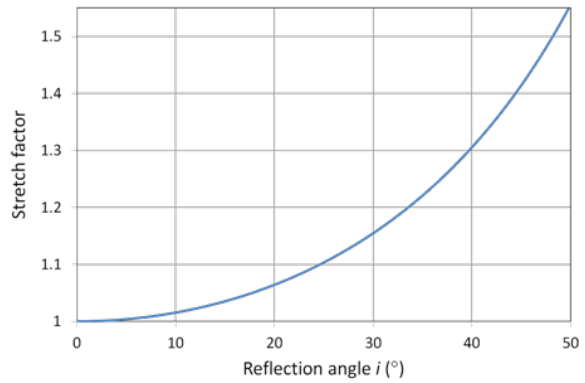

Figure 2 Stretch factor as function of reflection angle.

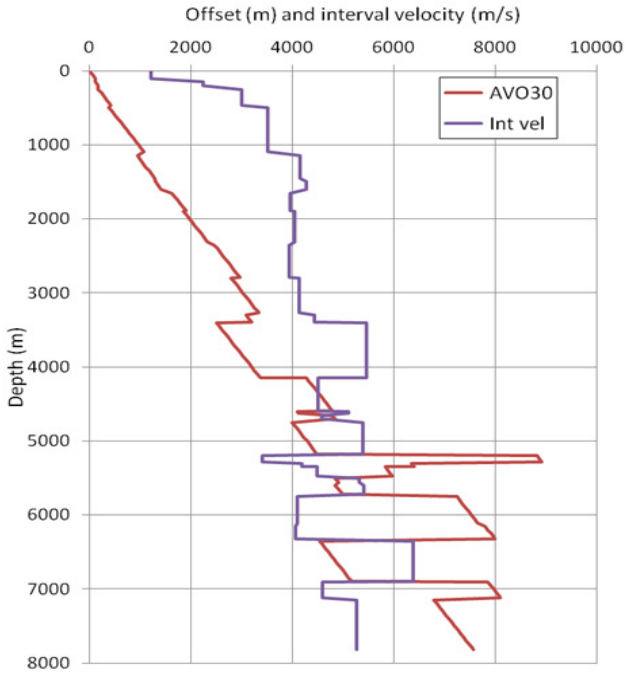

Figure 3 Interval velocity distribution for Region 1 and AVO offset required to illuminate horizontal reflectors with 30° angle of incidence. Note mirroring between the two curves.

The second condition in the first line of equation 2 ensures that the second square root stays real. Equation 2 for $\psi = 0$ applies also in case the variation of V_{rms} with t_0 is neglected.

Theoretically, the stretch factor for a reflection using a given shot/receiver combination can be computed from $S = 1/\cos i$, where i is the angle of incidence on the reflector for the shot/receiver pair (Levin, 1998 and others referenced by Levin). Figure 2 describes this relationship. It is of interest to link offset to angle i in a horizontally layered medium; this offset is twice the horizontal distance traveled by a ray starting with angle i from the layer of interest and ending at the surface. Next, this AVO offset can be compared to X_{mute} computed using equation 2 for $S_{max} = 1/\cos i$.

Figure 3 shows AVO offset for $i = 30°$ together with interval velocity as a function of depth. This figure illustrates that the AVO offset for high-velocity layers may be smaller than for shallower layers with lower interval velocities.

Figures 4, 5 and 6 show various mute offset graphs as function of time and depth for three different velocity distributions that are typical for a few places around the globe. Before the computations could be carried out, it was necessary to recompute the given velocity distributions for small increments in depth, so that dV_{rms}/dt_0 could be estimated reliably. For convenience, graphs for mute offsets computed without taking the dependence of V_{rms} on t_0 into account are labeled "old", whereas graphs that do take that dependence into account are labeled "new". The mute offsets have been computed for $S = 1/\cos i$ for $i = 30°$ and 40°. For the same values of i, also AVO offset is shown as AVO30 and AVO40.

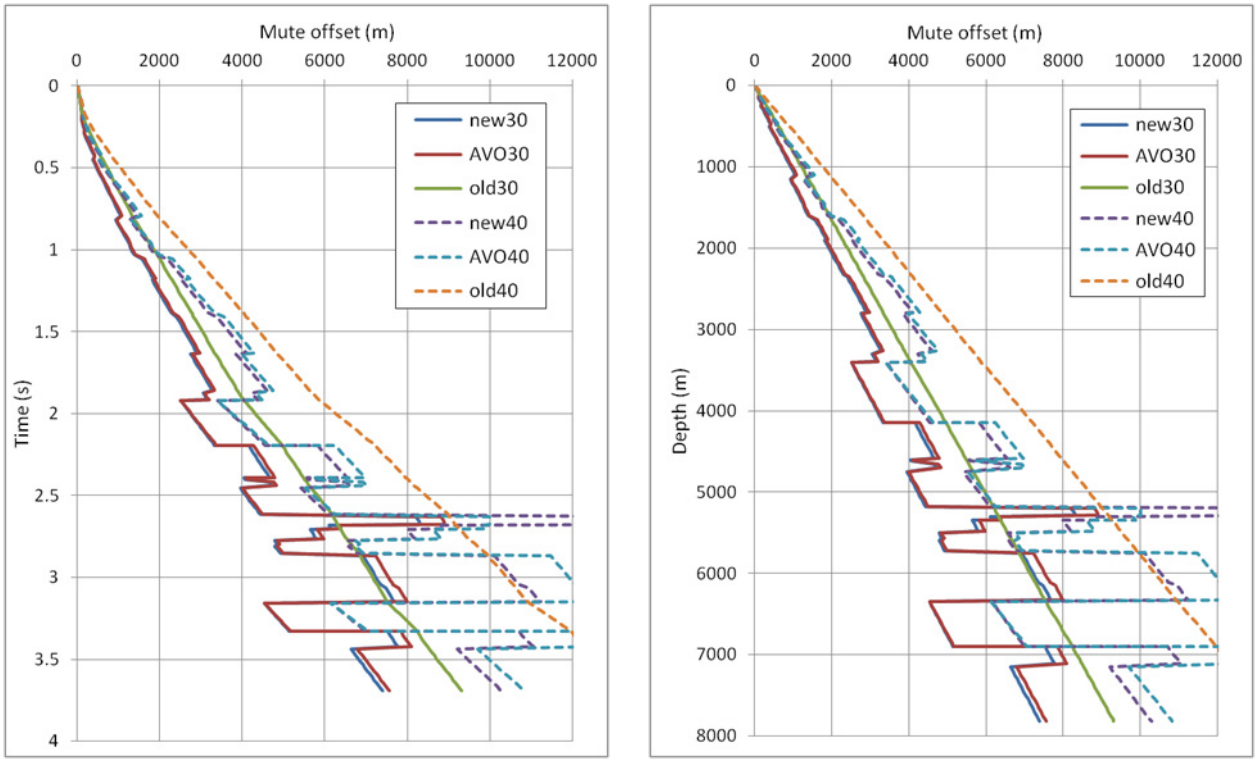

Figure 4 Mute offsets for Region 1 as function of traveltime (left) and depth (right). Curves labeled "new" are computed using equation 2 with $\psi \neq 0$, whereas curves labeled "old" are computed using equation 2 with $\psi = 0$. Curves labeled "AVO" represent offsets corresponding to a given incidence angle (30 or 40°). The stretch factor used for the "old" and "new" curves equals 1 / cos *i*, where *i* = 30 or 40°, i.e., $S \approx 1.15$ or 1.30 .

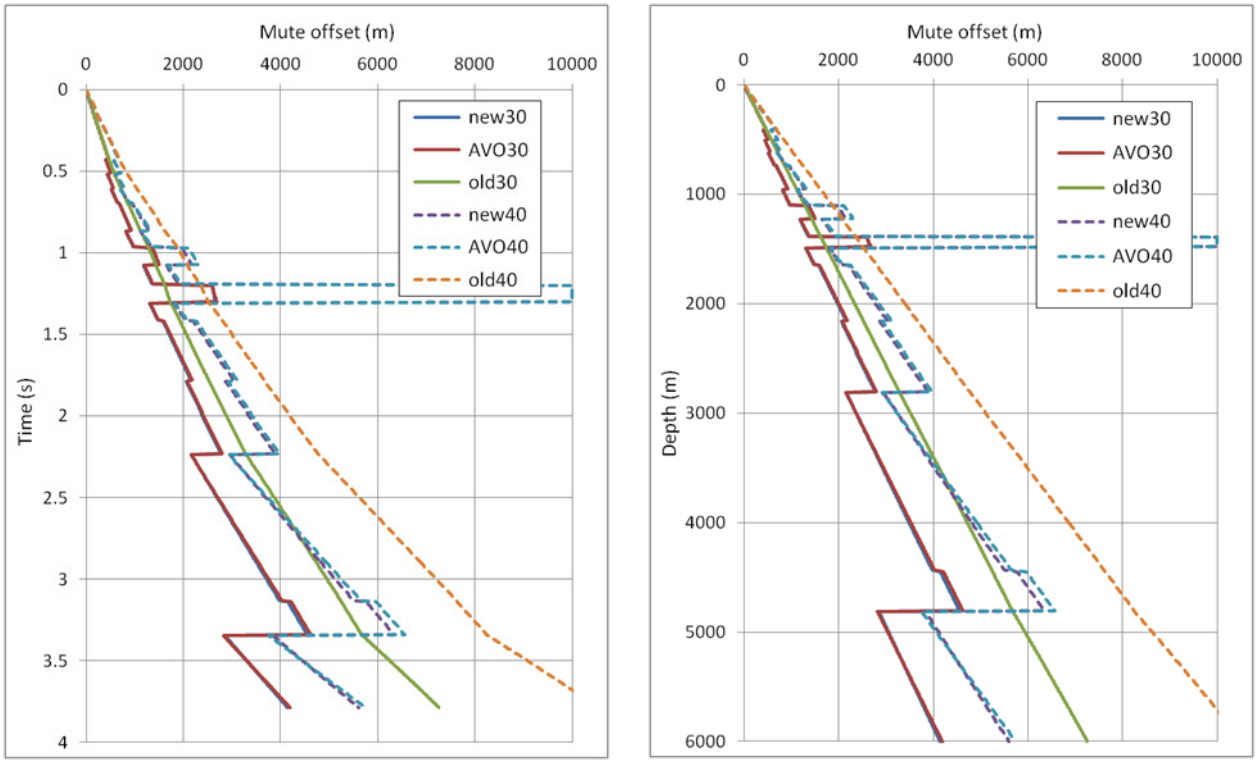

Figure 5 Same as Figure 4 for Region 2.

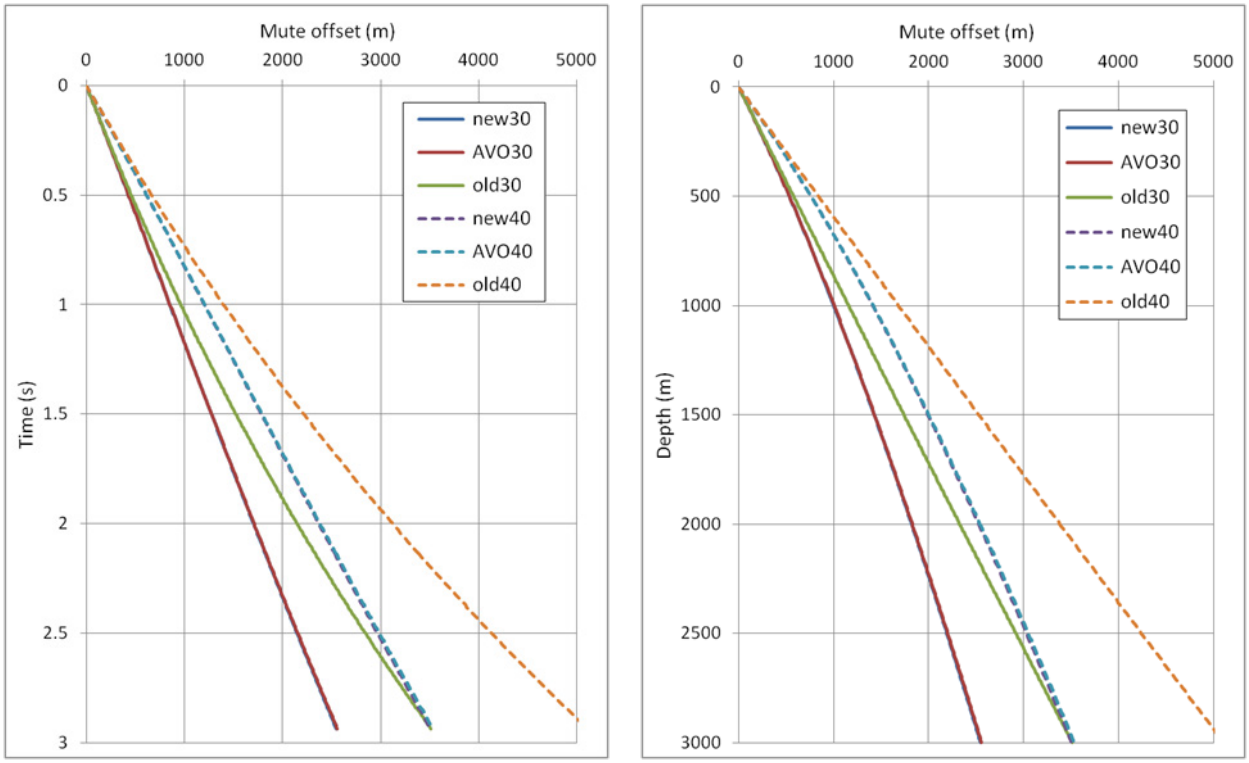

Figure 6 Same as Figure 4 for Region 3, which has velocity distribution V_{int} = 1500 + 0.4 z m/s, z is depth in m.

In all figures, the curves for "new" and "AVO' are virtually coinciding, whereas they have been computed in entirely different ways. It is a nice confirmation of theory that says that NMO stretch equals 1/cos i. In places where those curves differ from each other, this is caused by the assumption underlying equation 2, that the reflections are hyperbolas, whereas in actual fact reflection time also depends on higher orders of X^2. The curves labeled "AVO" are correct (assuming horizontal layering), because they are based on ray tracing. In Figure 6 the curves for "new" are hidden by the curves for "AVO". Here, the deviation of the reflection time functions from true hyperbolas must be very small.

Ray paths starting in layers with relatively low interval velocity may not reach the surface due to total reflection at an overlying high-velocity layer boundary. In Figure 4 this occurs for the layer around depth = 5250 m for i = 40°; for i = 30° the mute offset at that level is higher than for the "old30" curve. A similar phenomenon occurs in Figure 5 for depths around 1400 m.

The curves labeled "old" in Figures 4 - 6 correspond to $\psi = 0$ in equations 1 and 2. Equation 1 shows that S increases with increasing ψ. Similarly, equation 2 shows that X decreases with increasing ψ. Figure 7 illustrates the behavior of ψ for the three velocity distributions used in Figures 4 – 6. It shows that usually $\psi > 0$, leading to mute offsets that are smaller than computed with $\psi = 0$ in the curves labeled "old". Note that $\psi < 0$ around a depth of 6000 m in Region 1, leading to mute offsets that are larger than computed for $\psi = 0$ in Figure 4 for that level.

As a consequence of the usual increase of V_{rms} with t_0, the mute offsets are smaller than they are for $\psi = 0$. The effect tends to be largest for the deepest targets. Therefore, the maximum offset of the geometry might be chosen smaller than follows from the $\psi = 0$ curves. Before discussing this in more detail, it is useful to investigate the effect of $\psi > 0$ on average resolution.

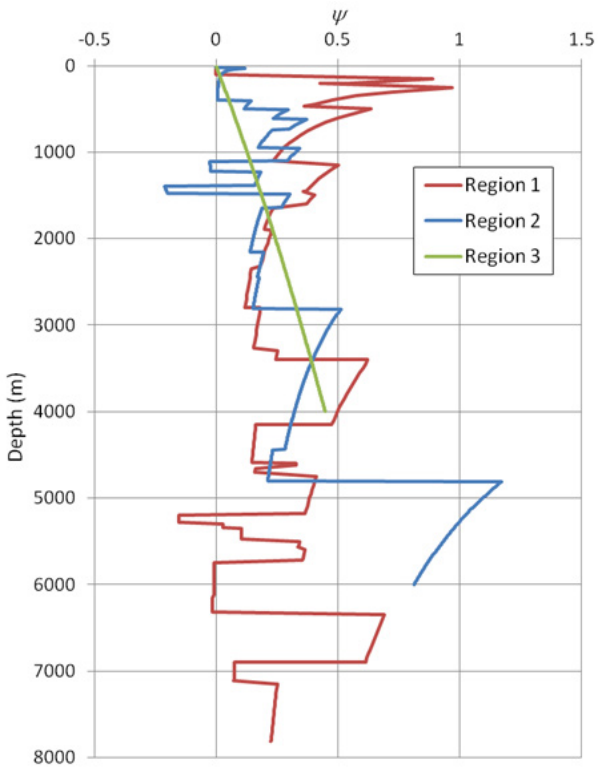

Figure 7 Behavior of $\psi = t_0/V_{rms}\ dV_{rms}/dt_0$ for the three different velocity distributions corresponding to Figures 4 – 6.

Average stretch factor

The maximum stretch factor is a measure of the NMO stretch occurring at the mute offsets; smaller stretch factors apply to smaller offsets with zero stretch at zero offset. Therefore, it is of interest to get some idea about the average stretch factor or the average loss of resolution (Vermeer, 2012). This quantity depends on the mix of offsets in the data; for the same maximum stretch factor and the same maximum offset, there is more loss of resolution due to NMO stretch for an offset distribution with relatively many long offsets than for an offset distribution with a constant offset trace density.

The following derives quantitative relations between average stretch effect and maximum stretch factor for a constant offset trace density as a function of offset (corresponding to a 2D offset distribution) and for an offset trace density that increases linearly with offset (as in wide-azimuth 3D offset distributions).

The wavenumber corresponding to each shot/receiver pair is reduced by cos i. The stretch factor in equation 1 is a good approximation of 1/cos i; therefore, to compute the effect of the mix of all offsets on wavenumbers or resolution, the average should be computed of $1/S$. The average value of $(1-\xi^2\psi)/\sqrt{1+\xi^2}$ for $0 \le \xi \le \xi_{max}$ is $(-\xi_{max}\sqrt{1+\xi_{max}^2}\psi + (2+\psi)ArcSinh(\xi_{max}))/(2\xi_{max})$. Hence, the average stretch factor for 2D data $S2D_{avg}$ follows from

$$S2D_{avg} = \frac{2\xi_{max}}{-\xi_{max}\sqrt{1+\xi_{max}^2}\psi + (2+\psi)ArcSinh(\xi_{max})} \qquad (3)$$

For the 3D case, offset trace density increases linearly with offset; hence the wavenumber contribution of each offset has to be weighted with (scaled) offset ξ, and the average value of ξ/S for $0 \le \xi \le \xi_{max}$ has to be computed in this case. This average value equals $2(-1+\sqrt{1+\xi_{max}^2} - (2+(-2+\xi_{max}^2)\sqrt{1+\xi_{max}^2})\psi/3)/\xi_{max}^2$, so that the average stretch factor for wide-azimuth 3D data $S3D_{avg}$ follows from

$$S3D_{avg} = \frac{\xi_{max}^2}{2(-1+\sqrt{1+\xi_{max}^2} - (2+(-2+\xi_{max}^2)\sqrt{1+\xi_{max}^2})\psi/3)} \qquad (4)$$

Taking $\xi = \xi_{max}$ in equation 1 links the maximum stretch factor via equation 3 to $S2D_{avg}$ and via equation 4 to $S3D_{avg}$. The average stretch factors for 2D and 3D data are plotted as a function of the maximum stretch factor in Figure 8 for three choices of ψ. If the aspect ratio of the acquisition geometry is not equal to 1, then the 3D curve would get closer to the 2D curve (for all times where the mute offset is larger than the smallest of maximum crossline and maximum inline offsets; for shallower levels the offset distribution is effectively circular, i.e., wide 3D coverage). Figure 8 shows that the effect of $\psi \neq 0$ on average stretch is not very strong.

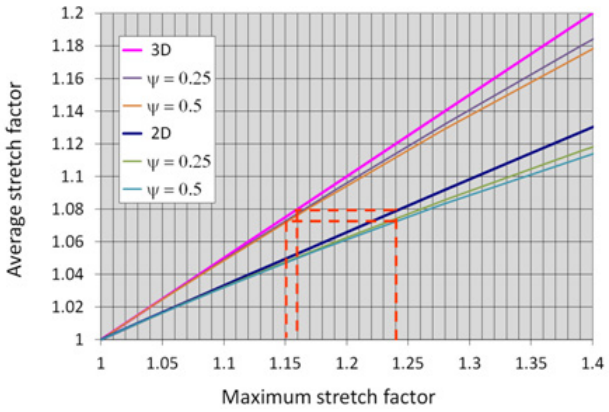

Figure 8 Average stretch factor as a function of maximum stretch factor for 2D and wide 3D data for three choices of ψ. The dashed red lines indicate that an average stretch of 7.5 to 8 % corresponds to a maximum stretch of 24 % in 2D data and 15 to 16 % in 3D data.

Obviously, the average stretch factor for 2D data is much smaller than the corresponding average stretch factor for 3D data. Interestingly, the two curves for $\psi = 0$ are virtually straight lines, which is not immediately obvious from equations 1, 3 and 4. Expansion of the expressions for $\psi = 0$ shows that if the maximum stretch factor is written as $1 + x$,

$$S2D_{\text{avg}} \cong 1 + x/3 \qquad (5)$$

and

$$S3D_{\text{avg}} \cong 1 + x/2 \qquad (6)$$

In 2D (see Figure 8), a maximum stretch factor of for instance 1.24 may be used to give an acceptable average stretch factor of 1.08. In 3D, the same maximum stretch factor would correspond to an average stretch factor of 1.12 leading to an extra loss in resolution which is not likely acceptable. For the same loss in resolution due to NMO, the 3D data should have a maximum stretch factor of 1.16 rather than 1.24, i.e., in processing a tighter mute function should be used for 3D data than for 2D data.

This tighter mute function for 3D data might also be applied in survey design, but it should be realized that accuracy of velocity determination and the ability to carry out AVO analysis are factors in favor of using a similar stretch factor in 3D as used in 2D.

Discussion

In areas with large dips, angles of incidence tend to be smaller as function of offset than in (sub)horizontally layered areas, thus allowing longer offsets for the same stretch. In such areas, equation 2 may still be used as a first guess of required mute offsets, perhaps multiplied with 1/cos (dip angle), but a ray-tracing exercise would be best for greater certainty.

The curves labeled "new" in Figures 4 - 6 show much more detail than the curves labeled "old". Therefore, the mute offsets computed using equation 2 are more sensitive to error than the curves that neglect the variation of V_{rms} with t_0. This greater sensitivity to error should be taken into account when using equation 2 in survey design.

Application of equation 2 with $\psi \neq 0$ for mute offset leads in general to smaller mute offsets than the $\psi = 0$ formula. This reflects the property that an increasing V_{rms} with t_0 leads to larger NMO stretch. The smaller mute offset may affect the choice of maximum offset of a geometry: given a maximum acceptable average stretch factor, the corresponding maximum mute offset for the deepest target might be used as guideline to choose maximum offset. However, this only applies in case the data are to be used just for structural interpretation.

In case AVO is to be applied to the final data, stretch factors have to be accepted that are much higher. In the past, simplified amplitude versus angle relationships were used that were valid up till 30°; Figure 2 shows that in that case a maximum stretch factor of 1.16 is sufficient to provide the offset range required for analysis. Nowadays, larger reflection angles are also used providing higher accuracy. For angles up to 40°, a maximum stretch factor of 1.3 has to be accepted. In case AVO analysis is planned for the deepest target, this large required maximum stretch factor leads to extra long offsets. In survey design this may be achieved by acquiring extra long offsets in one direction only (inline or crossline). These long offsets are to be used in AVO analysis and perhaps also in velocity analysis, but should not be used in structural imaging, because they would reduce resolution too much.

For azimuthal anisotropy analysis the same applies as for AVO: the larger offsets increase accuracy of the analysis. An important difference is that those large offsets are required for all azimuths; hence, a wide geometry with equally long inline and crossline offsets is required.

Full waveform inversion (FWI) benefits from the use of refractions. Useful refractions may extend beyond what would normally be termed very long offsets. The importance of very long offsets for FWI still needs further research and merits a close watch.

Survey design has to ensure that sufficiently long offsets are acquired. Processing must strike a balance between including more traces for better S/N, (potentially increasing resolution as well), and including only offsets with small enough stretch in the final migrated stacks.

Conclusions

For reflection traveltimes that can be approximated with a hyperbola, an accurate formula is now available for the computation of mute offset as a function of maximum NMO stretch. Without ray tracing, this offset also describes the offset required for AVO analysis.

Another formula describes the average stretch effect for a mix of offsets. What average stretch is acceptable depends on a balance between more traces (longer offsets) producing better S/N and better resolution and fewer traces (shorter offsets only) producing lower average stretch and better resolution.

References

Levin, S. A., 1998, Resolution in seismic imaging: Is it all a matter of perspective?: Geophysics, **65**, 743-749.

Vermeer, G. J. O., 1990, Seismic wavefield sampling: Society of Exploration Geophysicists.

Vermeer, G. J. O., 2012, 3D seismic survey design, Second edition: Society of Exploration Geophysicists.